Quiet zone generation in an acoustic free field using multiple parametric array loudspeakers

Jiaxin Zhong, Tao Zhuang, Ray Kirby, et al.

ARTICLES YOU MAY BE INTERESTED IN

JASA ARTICLE

Quiet zone generation in an acoustic free field using multiple parametric array loudspeakers

Jiaxin Zhong,[1,a)] Tao Zhuang,[2] Ray Kirby,[1,b)] Mahmoud Karimi,[1,c)] Haishan Zou,[2,d)] and Xiaojun Qiu[2,e)]

[1]*Centre for Audio, Acoustics and Vibration, University of Technology Sydney, New South Wales 2007, Australia*

[2]*Key Laboratory of Modern Acoustics, Institute of Acoustics, Nanjing University, Nanjing 210093, China*

ABSTRACT:

This paper investigates the feasibility of remotely generating a quiet zone in an acoustic free field using multiple parametric array loudspeakers (PALs). A primary sound field is simulated using point monopoles located randomly in a two-dimensional plane, or three-dimensional (3D) space, whereas the secondary sound field is generated by multiple PALs uniformly distributed around the circumference of a circle sitting on the same plane as the primary sources, or on the surface of a sphere for 3D space. A quiet zone size is defined as the diameter of the maximal circular zone within which the noise reduction is greater than 10 dB. The size of this quiet zone is found to be proportional to $0.19\lambda N$ for N secondary sources with a wavelength λ when the primary and secondary sources are in the same plane, whereas it is found to be $0.55\lambda N^{1/2}$ for the 3D case. The size of the quiet zones generated by PALs is similar to that observed with traditional omnidirectional loudspeakers; however, the effects of using PALs on the sound field outside the target zone is much smaller due to their sharp radiation directivity and slow decay rate along the propagation distance. Experimental results are also presented to validate these numerical simulations.
© 2022 Acoustical Society of America. https://doi.org/10.1121/10.0009587

I. INTRODUCTION

Generating a quiet zone in a noisy environment with active noise control (ANC) has been a research focus for several decades.[1–3] In recent years, progress has been made in areas such as reducing the number of microphones[4] and loudspeakers,[5] and enlarging the size of the quiet zone[6] as well as reducing computational complexity.[7] The sound pressure inside a closed surface surrounded by multiple secondary sources can be controlled if the spacing between the secondary sources is sufficiently small;[8] however, the sound field outside the target region might increase due to the sound generated by the secondary sources.[9,10] To address this problem, directional loudspeakers have been shown to have the potential to lower this external sound field.[10,11] Parametric array loudspeakers (PALs) have sharper directivity than most existing traditional loudspeakers,[12] but the feasibility of using them to create a large quiet zone is not clear, and so this will be investigated in this paper.

The challenge to be addressed with ANC involves maximizing the size of the quiet zone. For one secondary source, it is straightforward to reduce the noise at a single location; however, the size of the quiet zone is only about 1/10 of the wavelength in a diffuse sound field.[13,14] A larger quiet zone can be created by using multiple secondary sources surrounding the target region.[15] In a free field, the quiet zone size is proportional to the number of secondary sources.[9] Experimental measurements show that more than 20 dB of noise reduction can be obtained inside a sphere with a radius of 0.3 m for frequencies from 100 to 500 Hz, when using 30 secondary sources on a spherical surface.[16] In an ordinary room, experimental results with 16 secondary sources distributed over a cylindrical surface demonstrated that a cylindrical quiet zone with a height of 0.2 m and a radius of 0.2 m is possible below 550 Hz.[17] In these ANC systems, omnidirectional loudspeakers were used as secondary sources. Although the noise inside the target region is reduced, the sound pressure outside the region often increases, which is known as the spillover effect.[9,10] The noise amplification outside the target areas can be mitigated by optimizing some parameters, such as the separation between the secondary sources and the distance between secondary sources and error sensors.[9,18,19]

Directional sources can be used as secondary sources in multiple-channel ANC systems to improve performance. For example, tripole secondary sources with a cardioid radiation pattern have been used to reduce the primary source radiation.[20] Directional sources consisting of two closely located loudspeakers with pre-adjusted phase difference have also been used to increase the performance of an ANC barrier,[21] and directional sources consisting of a central circular core enclosed within an annulus have been used to control the noise generated by finite-length coherent line sources.[11] These directional secondary sources have been chosen because they radiate only in the direction of the target region, and so they have less effect on the other areas,

reducing the effects of noise amplification outside of the quiet zone.

PALs are an application of parametric acoustic arrays for radiating highly directional audio sound due to nonlinear interactions of ultrasonic waves in air. Since Brooks et al.,[22] a lot of work has been reported to implement PALs in ANC systems.[12] The advantage of using PALs in ANC systems has been shown for a single-channel system, where the noise at the target point is reduced without affecting sound fields in the surrounding area.[10,23,24] In Ref. 23, Komatsuzaki and Iwata also used simulation and experiment to show that the quiet zone size at 1 kHz is largest when the secondary source is placed between the error point and the noise source. Later, a two-channel ANC system using PALs was employed to reduce the binaural factory noise at human ears.[25] It was found that the crosstalk in the secondary paths is negligible, so the crosstalk cancellation technique is not required, resulting in a reduction in computational cost for the ANC controller. Based on their simulations, Tseng showed the quiet zone controlled by one or two PALs is larger than that controlled by traditional omnidirectional loudspeakers.[26] The reason observed was that the audible sound generated by the PAL decays slowly with distance, so the secondary field can more closely match the primary sound field. However, only a pure-tone low frequency at 108 Hz was considered in Ref. 26, and no measurement results were presented. There is little reported on the feasibility of using multiple (more than two) PALs as secondary sources to generate a larger quiet zone.

In this paper, the feasibility of generating a quiet zone in the free field with multiple PALs is investigated using simulations based on a quasilinear PAL radiation model.[27,28] Both two-dimensional (2D) and three-dimensional (3D) configurations are investigated, where the primary sources are assumed to be point monopoles located randomly on a 2D plane, or in 3D space. For a 2D problem, the secondary sources are uniformly distributed around the circumference of a circle on the same plane of primary sources. For a 3D problem, the secondary sources are uniformly distributed over a spherical surface. The relationship between the sound wavelength, the number of secondary sources, and the size of the quiet zone generated by the PALs is explored, and the influence of PALs on the sound field outside the quiet zone is discussed. Numerical simulations are also validated against experimental data.

II. THEORY

Figure 1 shows a schematic diagram of the ANC system to be investigated. The primary sources consist of N_p point monopoles randomly located on the xOy plane, or in 3D space. They are assumed to be harmonic with frequency f. The number of secondary sources is N_s, and they are uniformly distributed on a circle on the xOy plane, or a sphere with a radius of R_s, as shown in Figs. 1(a) and 1(b), respectively. For all cases, the target zone to be controlled is a 2D interior region of a circle on the xOy plane with a radius of R_0 centered at the origin of the Cartesian coordinate system O-xyz.

(a)

(b)
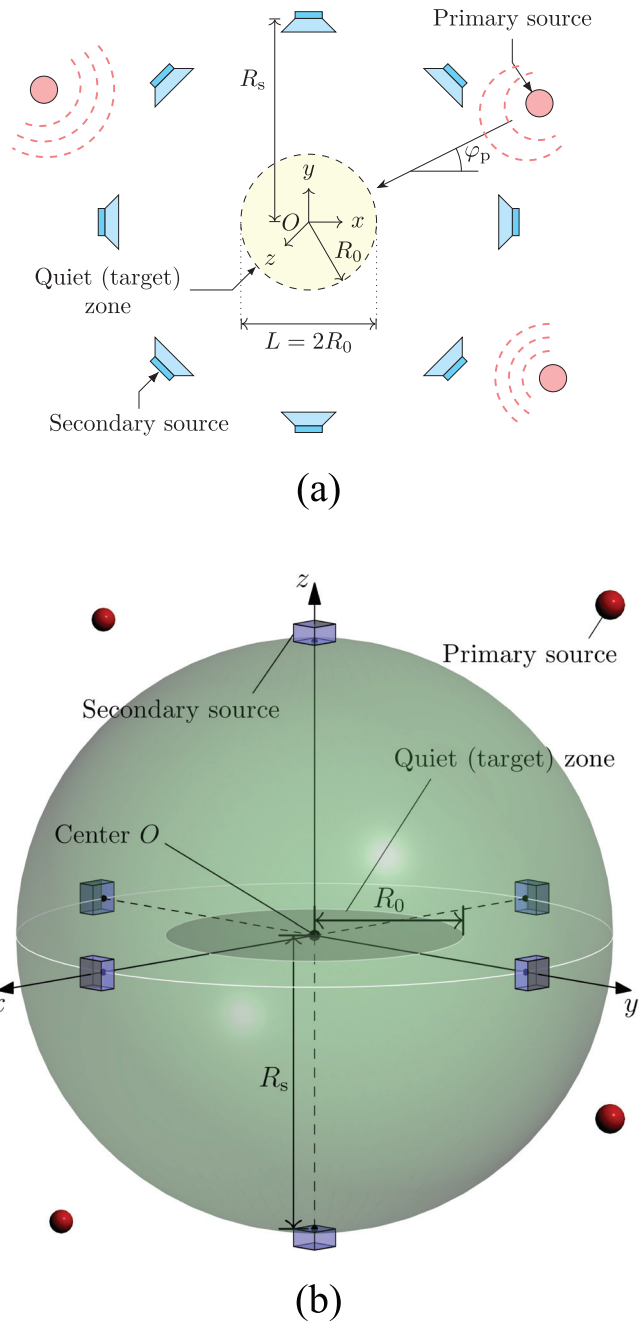
FIG. 1. (Color online) Schematic diagrams of an ANC system where the primary and secondary sources are located (a) on the xOy plane or (b) in 3D space.

The summation of the square of the sound pressure at each error point is chosen as the cost function for the ANC system, which yields[29,30]

$$J = \mathbf{p}_{et}^H \mathbf{p}_{et} + \beta \mathbf{Q}_s^H \mathbf{Q}_s, \qquad (1)$$

where $\mathbf{p}_{ep}$ and $\mathbf{p}_{es}$ are the sound pressure vectors at error points radiated by primary and secondary sources, respectively, and $\mathbf{p}_{et} = \mathbf{p}_{ep} + \mathbf{p}_{es}$. In addition, β is a real number to constrain the outputs of secondary sources,[29] $\mathbf{Q}_s = [Q_{s,1}, Q_{s,2}, \ldots, Q_{s,N_s}]^T$ is the source strength vector of the secondary sources, and the superscripts "T" and "H" denote the transpose and the conjugate transpose, respectively. The optimized source strengths of the secondary sources are[30]

$$\mathbf{Q}_{s,opt} = -(\mathbf{Z}_{es}^{H}\mathbf{Z}_{es} + \beta\mathbf{I})^{-1}\mathbf{Z}_{es}^{H}\mathbf{p}_{ep}, \tag{2}$$

where $\mathbf{Z}_{es}$ is an $N_e \times N_s$ matrix of the acoustic transfer functions from N_s secondary sources to N_e error points, and $\mathbf{I}$ is an identity matrix of size N_s. After obtaining the optimal secondary source strengths, the total sound pressure with control can be calculated.

In this paper, both traditional omnidirectional loudspeakers and PALs are adopted as secondary sources. The traditional loudspeakers are modeled as point monopoles, where the sound pressure is given as

$$p(\mathbf{r}) = -i\rho_0\omega Q_0 \frac{e^{ik|\mathbf{r}-\mathbf{r}_0|}}{4\pi|\mathbf{r}-\mathbf{r}_0|}, \tag{3}$$

where i is the imaginary unit, ρ_0 is the air density, $\omega = 2\pi f$ is the angular frequency, $k = \omega/c_0$ is the wavenumber, Q_0 is the source strength, and $|\mathbf{r} - \mathbf{r}_0|$ is the distance between the field point $\mathbf{r}$ and the source point $\mathbf{r}_0$.

A quasilinear solution of the Westervelt equation is adopted here because previous studies have demonstrated its validity when PALs are operated with the parameters used in this paper.[27,28,31,32] The audio sound pressure radiated by a PAL can be considered as a superposition of the pressure radiated by infinite virtual sources in air with the source density function proportional to the sound pressure of ultrasound. This can be calculated as

$$p(\mathbf{r}) = -i\rho_0\omega v_1 v_2^* \iiint_V q(\mathbf{r}_v) \frac{e^{ik|\mathbf{r}-\mathbf{r}_v|}}{4\pi|\mathbf{r}-\mathbf{r}_v|} d^3\mathbf{r}_v, \tag{4}$$

where v_1 and v_2 are the amplitude of the vibration velocity on the transducer surface for the ultrasound f_1 and f_2 ($f_1 > f_2$), respectively. Furthermore, the PAL is assumed to be placed at the origin and radiates in the positive axial direction, where the superscript "*" denotes the complex conjugate, the integration range V represents the whole 3D space, and $v_1 v_2^* q(\mathbf{r}_v)$ is the source density function at the virtual source point $\mathbf{r}_v$ determined by the ultrasound pressure. The radiated audio sound pressure can be tuned by controlling the values of v_1 and v_2 of the ultrasound, so that $v_1 v_2^*$ is defined as the source strength of a PAL, which is equivalent to Q_0 in Eq. (3).

To investigate the performance of the ANC system, the sound pressure in a large square region with dimensions of $-2\,\text{m} \le x \le 2\,\text{m}$, and $-2\,\text{m} \le y \le 2\,\text{m}$ and its center at the origin O, is calculated for all cases. A mesh of squares in this region is generated with a separation between grid points no larger than 1/20 of wavelength. All grid points are chosen as evaluation points, whereas only the ones inside the circular target zone are chosen as the error points.

The noise reduction (NR) inside the circular target zone is defined as

$$\text{NR} = 10\log_{10}\left(\frac{\mathbf{p}_{ep}^{H}\mathbf{p}_{ep}}{\mathbf{p}_{et}^{H}\mathbf{p}_{et}}\right) \ (\text{dB}). \tag{5}$$

The NR decreases as the radius of the circular target zone increases, so that the size of the quiet zone L is defined as

the diameter of the maximal target zone satisfying that the NR is greater than 10 dB.

To evaluate the spillover effect of secondary sources on the surrounding areas quantitatively, a measure called "potential energy gain" is defined as

$$G = 10\log_{10}\left(\frac{\mathbf{p}_{vt}^{H}\mathbf{p}_{vt}}{\mathbf{p}_{vp}^{H}\mathbf{p}_{vp}}\right) \ (\text{dB}), \tag{6}$$

where $\mathbf{p}_{vp}$ and $\mathbf{p}_{vs}$ are the sound pressure vectors at evaluation points radiated by primary and secondary sources, respectively, and $\mathbf{p}_{vt} = \mathbf{p}_{vp} + \mathbf{p}_{vs}$. Equation (6) is similar to the definition for NR given by Eq. (5) and defines the change in the acoustic potential energy in the square region after control, so that $G > 0$ represents a gain, and $G < 0$ a reduction, in the acoustic potential energy.

III. SIMULATIONS

Two configurations of secondary sources are considered in this section. The 2D configuration denoted in Sec. III A is shown in Fig. 1(a), where N_s secondary sources ($N_s = 8$ in the figure) are evenly placed on a circle and the azimuthal angle at the ith source is $\varphi_{s,i} = 2\pi (i-1)/N_s$, $i = 1, 2, \ldots, N_s$. The 3D configuration denoted in Sec. III B is shown in Fig. 1(b), where N_s secondary sources ($N_s = 6$ in the figure) are evenly placed on a spherical surface and the minimal distance between two arbitrary secondary sources is denoted by d_{min}. The secondary source locations are obtained by maximizing d_{min}, and the source coordinates for different N_s can be found in Ref. 33. The radius of the secondary source array is set to be $R_s = 1.5$ m in all of the simulations that follow.

The quiet zone size, L, is obtained by using an iterative procedure. The initial lower (R_1) and upper (R_2) values are set to 0 and 1.5 m, respectively. The NR inside the circular target zone is calculated when the radius of the target zone R_0 is set as $(R_1 + R_2)/2$. If NR < 10 dB, the upper value R_2 is updated as $(R_1 + R_2)/2$. If NR > 10 dB, the lower value R_1 is updated as $(R_1 + R_2)/2$. The iteration stops when $(R_2 - R_1)$ is less than 1/20 of the wavelength and $(R_1 + R_2)$ is chosen as the quiet zone size L. All simulation results presented in this paper have followed this procedure.

Each PAL is assumed to be circular with a radius of 0.1 m and a uniform surface velocity profile for the ultrasound. The carrier frequency for ultrasound affects the audio sound generated by a PAL, and it usually ranges from 40 to 70 kHz. At lower frequencies, the directivity is sharper and the audio sound pressure decays more slowly with respect to the propagation distance because the effective length of the virtual source array is larger at smaller absorption coefficients.[34] Because the carrier frequency of the commercial PALs used in the experiments is 64 kHz, this frequency is also used in the simulations. The Rayleigh distance is then 5.86 m at 64 kHz. The sound attenuation coefficients at both ultrasonic and audio sound frequencies are calculated according to International Organization for Standardization

J. Acoust. Soc. Am. **151** (2), February 2022

Zhong *et al.* 1237

9613-1 with a relative humidity of 60% and a temperature of 25 °C.[35] The sound attenuation coefficient at 64 kHz is $\alpha_u = 0.29$ Np/m, so the absorption distance is 1.72 m calculated by $1/(2\alpha_u)$.[34] The audio sound generated by each PAL is calculated using the spherical expansion method proposed in the authors' previous works.[27,32] The accuracy of the calculation method has been validated by experiment[36] and is discussed in detail in Refs. 31 and 32.

A. 2D secondary source array

Figure 2 shows the primary and total sound fields at 1 kHz under the optimal control by eight PALs, or point monopoles, shown as black rectangles or circles, respectively, where the primary source (not shown in the figure) is a single monopole located at an azimuthal angle of $\varphi_p = 22.5°$ with a distance to the origin of 4 m. The angle of 22.5° is selected because it is the angle of the bisector of the first and second secondary sources, which is the worst case for NR performance.[30] The quiet zone size in Figs. 2(b) and 2(c) is 0.45 and 0.46 m, respectively. Although the quiet zone sizes are similar, the potential energy gain associated with the point monopole sources is 6.9 dB, which is much larger than the −0.1 dB obtained with the PALs. The decrement of energy is mainly contributed from the noise reduction in the quiet zone, and it is roughly the same for both kinds of loudspeakers. The sound pressure around the traditional loudspeakers located on the direction of the primary source is large, so that the noise amplification can be clearly observed, and this amplification is observed to be present outside the radiation direction from these sources toward the quiet zone. However, it is not observed when using PALs, because they generate unidirectional secondary waves and these waves decay slowly along the propagation path. This is the reason the potential energy gain is much smaller when using PALs than when using traditional loudspeakers.

Figure 3 shows the quiet zone size and the potential energy gain as a function of the azimuthal angle of a primary source 4 m away from the origin at 1 kHz for a various number of secondary sources. The peaks and valleys in Figs. 3(a) and 3(b) are associated with the location of the secondary sources. It is clear that the quiet zone size increases when the primary wave angle approaches that of the secondary source, which is due to better matching of the wave

fronts from the primary and secondary sound waves.[9] In most cases, when there is one secondary source, the difference between the size of the quiet zone for the PAL and the point monopole secondary sources is less than 10% when the primary source angle is greater than 20°. The minimal quiet zone size is also 0.035 m when the primary source angle is at 180°, and the size is about 1/10 of the wavelength.

It is shown in Fig. 3 that increasing the secondary source number enlarges the size of the quiet zone. For example, the minimal quiet zone size is 0.035 m, 0.2 m, 0.46 m, and 0.97 m when the secondary source number is 1, 4, 8, and 16, respectively. The primary source azimuthal angles with minimal quiet zone sizes are the ones with their bisector between two adjacent secondary sources. Although the quiet zone size created by both PAL and point monopole secondary sources are approximately the same in most cases, the potential energy gain caused by the point monopoles are generally above 6 dB, which is larger than the one caused by PALs, which is around 0 dB.

To understand the performance of the ANC systems under complex acoustic environments, in the next examples, eight primary sources are placed on the same plane of the secondary source array, where the distance between each primary source and the origin is randomly and uniformly set between 3.5 and 4.5 m; the azimuthal angle is randomly and uniformly set between 0 and 360°; the source strength is randomly and uniformly set between 0.75×10^{-4} and 1.25×10^{-4} m³/s; and this configuration is denoted here as "2D primary sound field". Figure 4 shows the results of one trial of the 2D primary sound field, and the total sound field controlled by eight secondary sources. The quiet zone size created by both sources is 0.53 m, while the potential energy gain is −0.2 dB with the PALs and 6.5 dB with the point monopoles.

Figure 5 shows the quiet zone size and the potential energy gain based on 100 trials of random 2D primary sound fields generated by eight point monopoles randomly located on the xOy plane. The quiet zone size decreases as the frequency increases in all cases and is about 0.75λ, 1.5λ, and 3λ under optimal control conditions with four, eight, and sixteen point monopoles, respectively, where λ is the wavelength of the sound at the corresponding frequency. The quiet zone size generated by the point monopoles is larger
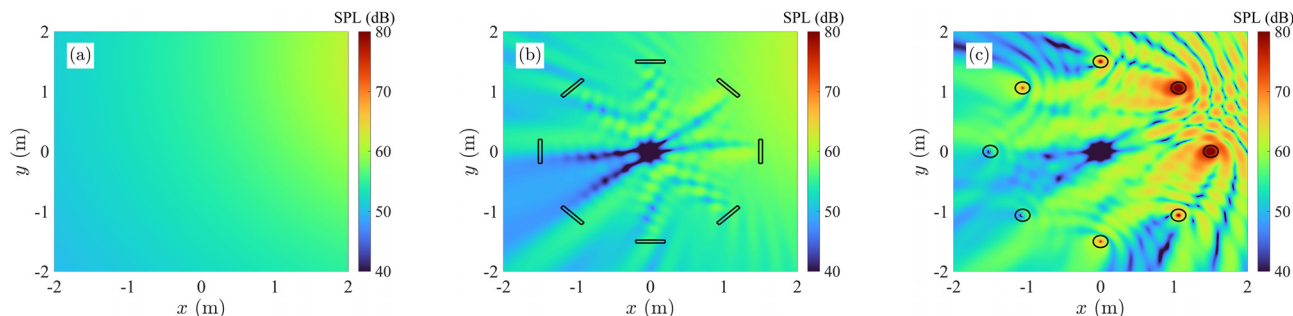

FIG. 2. (Color online) The sound field at 1 kHz (a) for the primary noise comes from $\varphi_p = 22.5°$, (b) under the optimal control with eight PALs, and (c) under the optimal control with eight point monopoles.
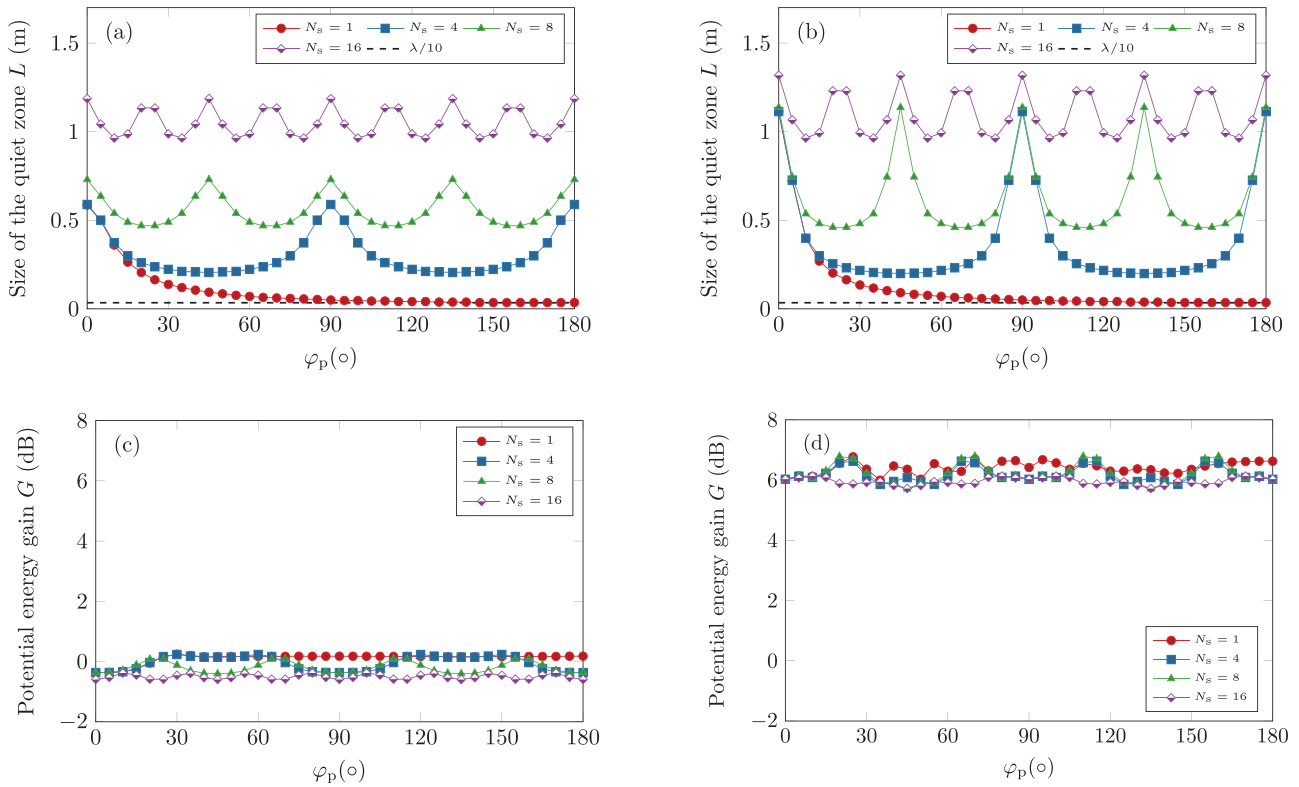
FIG. 3. (Color online) The quiet zone size and the potential energy gain as a function of the primary source azimuthal angles at 1 kHz for different numbers of secondary sources: (a) and (b) the quiet zone size created by PALs and point monopoles, respectively; (c) and (d) the potential energy gain caused by PALs and point monopoles, respectively. Red circles, $N_s = 1$; blue squares, $N_s = 4$; green triangles, $N_s = 8$; purple diamonds, $N_s = 16$; and dashed line, $\lambda/10$.

than the one generated by PALs, especially at the low frequencies; however, the difference between them becomes negligible at the middle and high frequencies. For example, the quiet zone sizes are 1.33 and 1.21 m respectively for eight monopoles and PALs at 400 Hz, whereas both become about 0.55 m at 1 kHz. The potential energy gain caused by the point monopoles is always larger than the one caused by the PALs, which increases only slightly as the frequency increases.

Figure 6 shows the quiet zone size and the potential energy gain at different numbers of secondary sources at 1 and 2 kHz. It is clear that the quiet zone size increases as the number of secondary sources increases. When the secondary source number becomes large, the quiet zone size increases slowly due to the limitations of the size of secondary source array (3 m) and the narrow beam width of the sound radiated by

PALs. As shown in Fig. 6(a), when the secondary source number is, respectively, less than 20 and 48 at 1 and 2 kHz, the quiet zone size is approximately proportional to the secondary source number and can be estimated by the following formula:

$$L = 0.19\lambda N_s. \tag{7}$$

For the ANC systems with N_s secondary sources, the arc length between adjacent secondary sources can be obtained by dividing the circumference of the generated quiet zone to give a length of $\pi L/N_s$. Using the L value in Eq. (7), the arc length is about 0.6λ, which indicates that the separation between the secondary sources is about 1/2 of the wavelength. This agrees with the remarks in Refs. 30 and 37. Figure 6(b) shows that the potential energy gain can also be reduced by introducing more
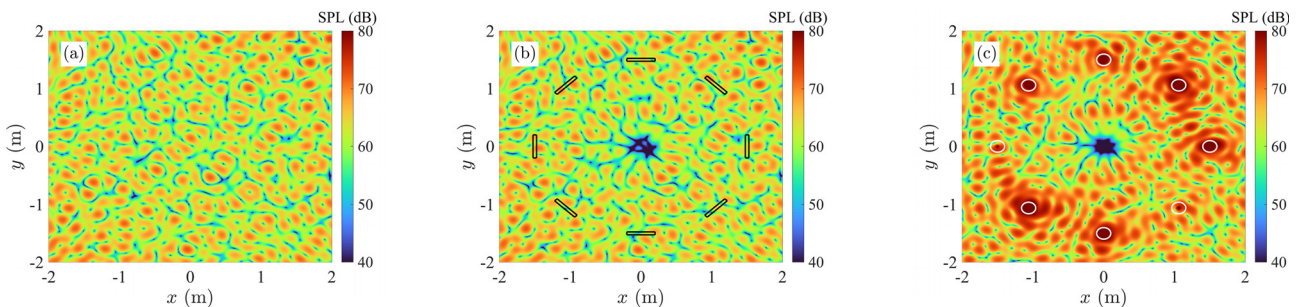

FIG. 4. (Color online) The sound field at 1 kHz (a) generated by eight point monopoles randomly located on the xOy plane, (b) under the optimal control with eight PALs, and (c) under the optimal control with eight point monopoles.

J. Acoust. Soc. Am. **151** (2), February 2022
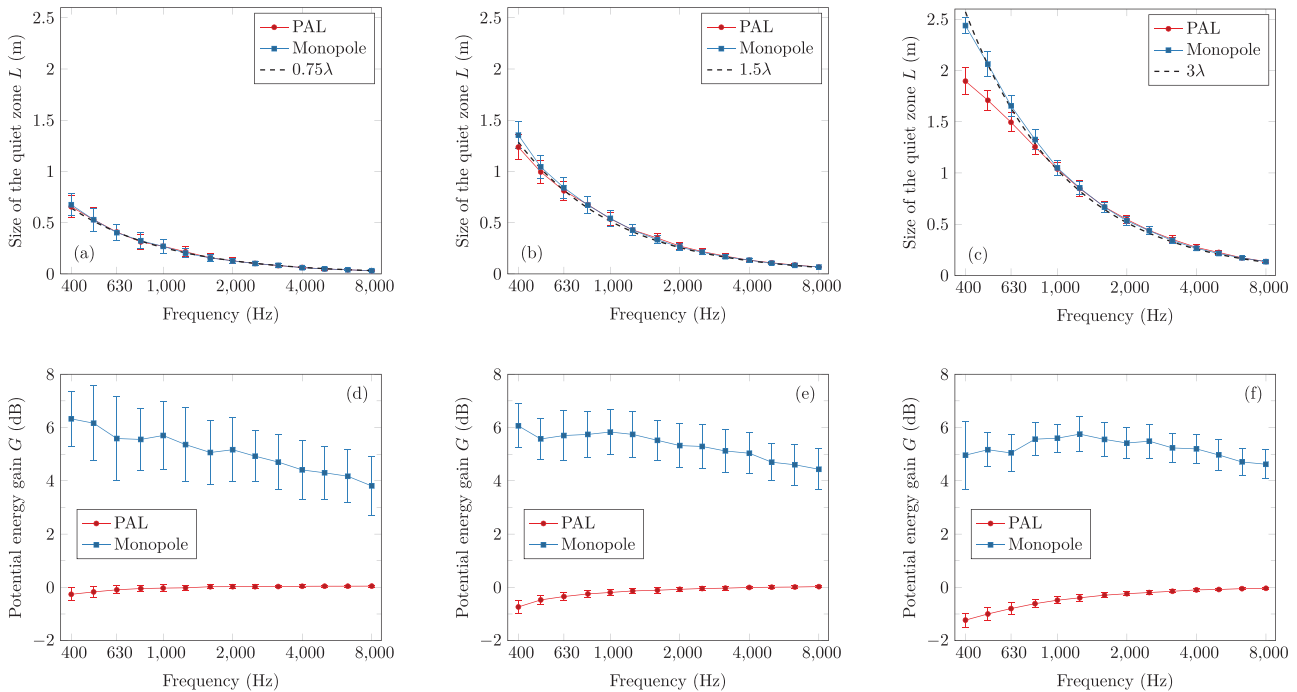
Zhong *et al.* 1239

FIG. 5. (Color online) For random 2D primary sound fields under the optimal control with the 2D secondary sources: (a), (b), and (c) the quiet zone size when the secondary source number is 4, 8, and 16, respectively; and (d), (e), and (f) the potential energy gain when the secondary source number is $N_s = 4$, 8, and 16, respectively, where the value and error bar are the mean value and standard deviation of 100 random trials, and λ is the wavelength. Red circles, PAL; blue squares, monopole; dashed lines, 0.75λ, 1.5λ, and 3λ for (a), (b), and (c), respectively.

secondary sources and the reduction is more significant at lower frequencies.

In the following simulations, the primary noise comes from multiple directions in 3D space, and the configuration is denoted by "3D primary sound field", although the secondary sources are still located on the 2D xOy plane. Figure 7 shows the quiet zone size and the potential energy gain based on 100 random trials of 3D primary sound fields under the optimal control of eight secondary sources in the xOy plane. Compared with Fig. 5(b), the mean value of the quiet zone size decreases from 1.5λ to 0.75λ, whereas the standard deviation shows no significant changes. Compared with Fig. 5(e), the potential energy gain caused by the PALs becomes positive at most frequencies, whereas it is still much smaller than the one caused by the point monopoles.

Figure 8 shows the quiet zone size and the potential energy gain based on 100 random trials of 3D primary sound fields using different numbers of 2D secondary sources. When the secondary source number N_s is small, the quiet zone size increases as N_s increases, but it changes slightly when $N_s > 10$. At 1 kHz, the quiet zone size generated by using the point monopoles and PALs approaches 0.29 and 0.27 m, respectively, at large secondary source numbers. At 2 kHz, the quiet zone size approaches 0.14 m. The maximal quiet zone size is about 0.75λ no matter how many secondary sources are used. When $N_s < 8$, the quiet zone size can be estimated as

$$L = 0.095\lambda N_s, \qquad (8)$$

which is 1/2 of that in Eq. (7). The reason for having a small quiet zone size is that the primary noises coming out of the xOy plane cannot be effectively controlled and because of that fact no secondary sources are placed in these directions. Furthermore, the potential energy gain caused by both types of secondary sources decreases with an increasing number of secondary sources, as shown in Fig. 8(b).

B. 3D secondary source array

Figure 9 shows the quiet zone size and potential energy gain when random 3D primary sound fields are optimally controlled by 8 and 20 secondary sources located in 3D space at different frequencies. Compared with Fig. 7(a), the quiet zone size increases from 0.75λ to λ by using a 3D instead of 2D secondary source array, even with the same number of secondary sources ($N_s = 8$). Therefore, the quiet zone size is not limited by 0.75λ, as was the case for 2D secondary sources, but may be increased to 2.2λ when the secondary source number is 20. For the monopoles, although the quiet zone is enlarged, the potential energy gain is also increased, this time by more than 2–4 dB as the number of secondary sources increased from 8 to 20 as shown in Fig. 9(b).

Figure 10 shows the quiet zone size and potential energy gain when random 3D primary sound fields are optimally controlled by the 3D secondary source array at 1 and 2 kHz. The quiet zone size is observed to be approximately proportional to the square root of the secondary source number and can be estimated by

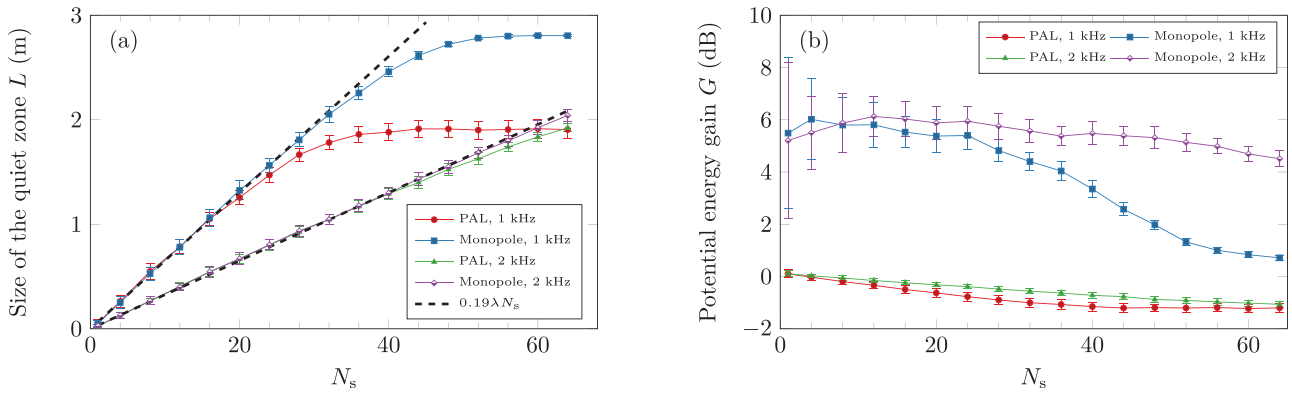$$L = 0.55\lambda\sqrt{N_s}, \qquad (9)$$

FIG. 6. (Color online) For random 2D primary sound fields under the optimal control with 2D secondary sources at 1 and 2 kHz: (a) the quiet zone size as a function of secondary source number; and (b) the potential energy gain as a function of secondary source number. Red circles, PAL at 1 kHz; blue squares, monopole at 1 kHz; green triangles, PAL at 2 kHz; purple diamonds, monopole at 2 kHz.

at all cases when the secondary source number N_s is less than 120. To control the 3D primary sound field, the secondary sources are distributed evenly on a spherical surface. Suppose there is a smaller sphere with a diameter of L centered at the origin and enclosed by the secondary source array. The area of this sphere divided by N_s is $\pi L^2/N_s$, and by using the value for L from Eq. (9), the area that can be controlled by each secondary source is then $0.95\lambda^2$. In other words, the size of the area controlled by each secondary source is about one wavelength. As for the potential energy gain, the value when using the monopoles varies significantly at different secondary source numbers, whereas the value when using the PALs is much smaller for both the mean value and standard deviation.

IV. EXPERIMENTS

The experiments were conducted in a full anechoic room at Nanjing University with dimensions of 11.4 m × 7.8 m × 6.7 m (height). The sketch and photo of the experimental setup and equipment are shown in Figs. 11 and 12, respectively. All equipment was placed at the same height. Four commercial PALs (Audio Spotlight AS-16i, Holosonics, Watertown, MA) were used and evenly located on a circle with a radius of 2.2 m, which is a 2D

configuration with four secondary sources, as discussed in Sec. III A. The PAL has a surface size of 0.4 m × 0.4 m and a carrier frequency of 64 kHz. Four laboratory-made traditional loudspeakers with dimensions of 20.7 cm × 18.7 cm × 11.6 cm were used as primary sources, and they were placed on a circle with a radius of 2.5 m.

An error microphone array was placed at the center with a size of 0.55 m × 0.55 m and a grid separation of 0.05 m. All microphones are electret microphones with a sensitivity of about 30 mV/Pa and are of the same type BAST M1212 (No. 23 Xixiaofu, Haidian, Beijing) calibrated with a Brüel & Kjær 4231 (Skodsborgvej 307, 2850 Nærum, Denmark) calibrator. The sound pressure at microphones was sampled with a Brüel & Kjær PULSE system (the analyzer 3053-B-120 equipped with the front panel UA-2107–120). The fast Fourier transform analyzer in PULSE LabShop was used to obtain the fast Fourier transform spectrum. The frequency span was set to 6.4 kHz, with 6400 lines, and the averaging type was linear with 66.67% overlap and 30 s duration. All microphones were covered by a piece of small and thin plastic film to avoid spurious sound.[38] Preliminary measurements show the insertion loss of this plastic film is more than 30 dB at 64 kHz, which is sufficient to isolate the intensive ultrasound.
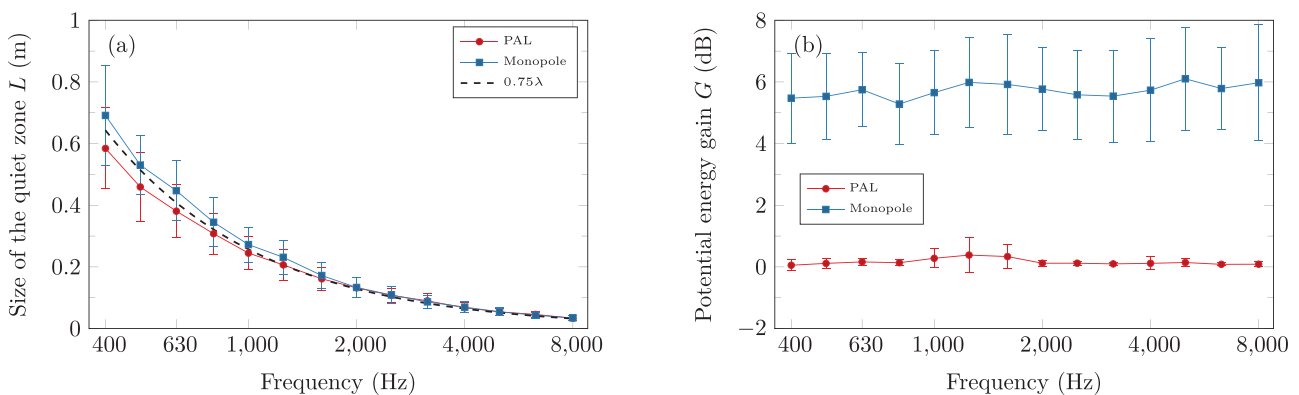

FIG. 7. (Color online) For random 3D primary sound fields under the optimal control with eight 2D secondary sources in the plane xOy, (a) the quiet zone size as a function of frequency; and (b) the potential energy gain as a function of frequency. Red circles, PAL; blue squares, monopole; dashed line, 0.75λ.

J. Acoust. Soc. Am. **151** (2), February 2022
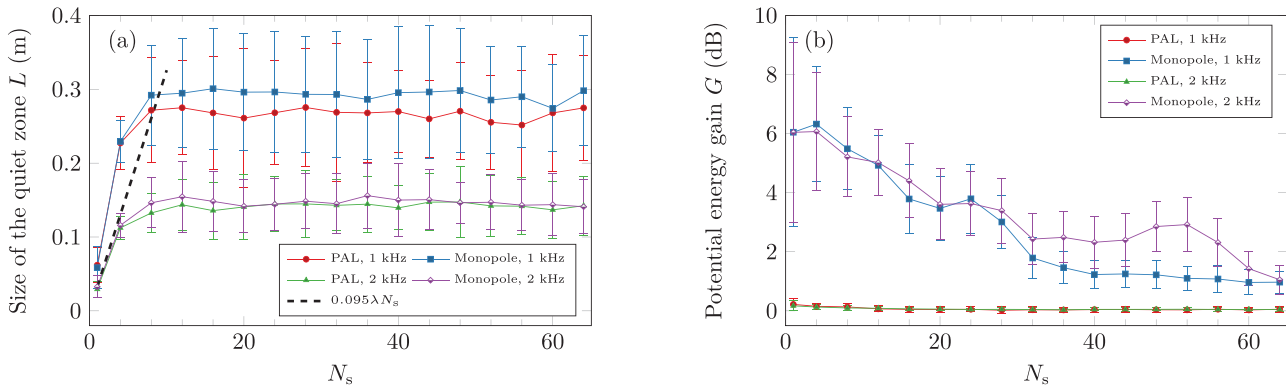
Zhong et al.   1241

FIG. 8. (Color online) For random 3D primary sound fields controlled by 2D secondary sources at 1 and 2 kHz: (a) the quiet zone size as a function of the secondary source number; and (b) the potential energy gain as a function of the secondary source number. Red circles, PAL at 1 kHz; blue squares, monopole at 1 kHz; green triangles, PAL at 2 kHz; purple diamonds, monopole at 2 kHz; dashed line, $0.095\lambda N_s$.

A laboratory-designed and -made ANC controller (Antysound Tiger ANC Pro-M, 20–203 Guangzhou Rd., Nanjing, China) was used with a multicore digital signal processor (TMS320C6678F, Texas Instruments, Dallas, TX). All error microphones used in experiments were connected into the ANC controller via a multichannel preamplifier. The output signals for the secondary sources were calculated based on a multichannel FxLMS algorithm and fed into the PALs directly. The primary sources were played with pure-tone sound, and the signal was also fed to the controller as the reference signal.

The quiet zone size in the experiments was determined as follows. First, simulations were used to estimate the quiet zone size in Fig. 11. Second, all microphones inside this circle were connected to the controller as the error sensors. When the number of microphones exceeds 24, only 24 were selected and then uniformly distributed with a separation of adjacent microphones no less than 1/6 of the wavelength. This trade-off is because of the limitations of the number of input channels available and the computational ability of the controller. Third, a tonal primary sound field was generated,

and the ANC process started. Finally, if the measured noise reduction at these microphones was less (or larger) than 10 dB, the size was decreased (or increased) a small amount until a quiet zone size was found where the noise reduction was close to 10 dB.

Figure 13 compares the experimental measurements with predictions obtained using Eq. (7) for two and four PALs as secondary sources, at 1/3 octave center frequencies from 400 Hz to 4 kHz. It can be seen that the experimental results are generally in accordance with predictions from 500 Hz to 4 kHz. It demonstrates that PALs are able to create a quiet zone in real multichannel ANC systems like traditional loudspeakers. The measured quiet zone size at low frequencies is lower than expected. For example, the measured size is 0.27 and 0.48 m at 400 Hz with two and four PALs, respectively, which is lower than the predicted 0.32 and 0.65 m. This might be caused by the poor low-frequency response of the PAL. The measured size above 630 Hz is usually slightly larger than predictions with four PALs. This might be because only four primary sources were used in the experiments, which is not ideal to simulate a random primary sound field. The measured
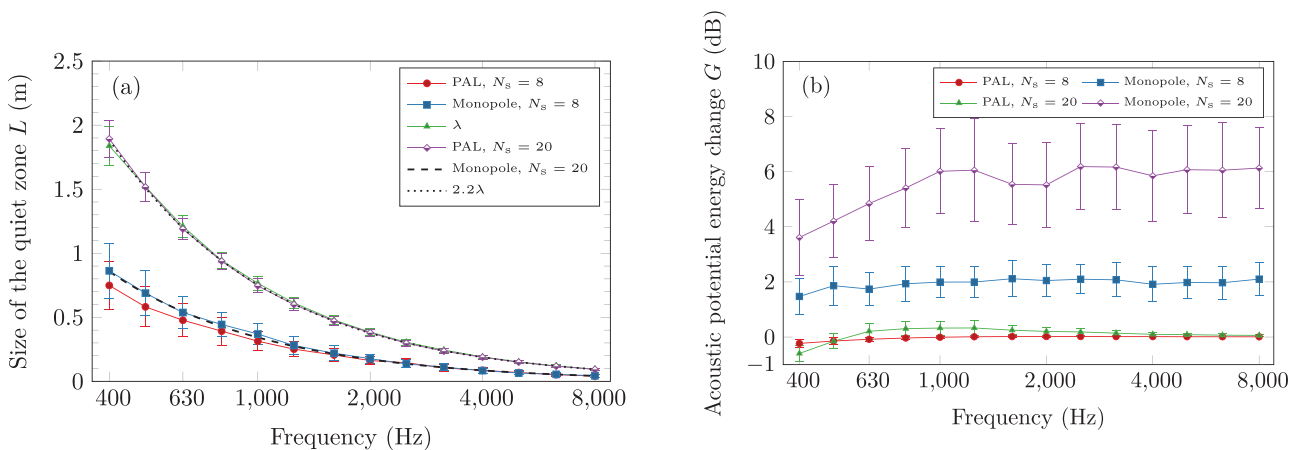

FIG. 9. (Color online) For random 3D primary sound fields under the optimal control with the 3D secondary sources: (a) the quiet zone size as a function of frequency; and (b) the potential energy gain as a function of frequency. Red circles, PAL when $N_s = 8$; blue squares, monopole when $N_s = 8$; green triangles, PAL when $N_s = 20$; purple diamonds, monopole when $N_s = 20$; dashed line, λ; dotted line, 2.2λ.
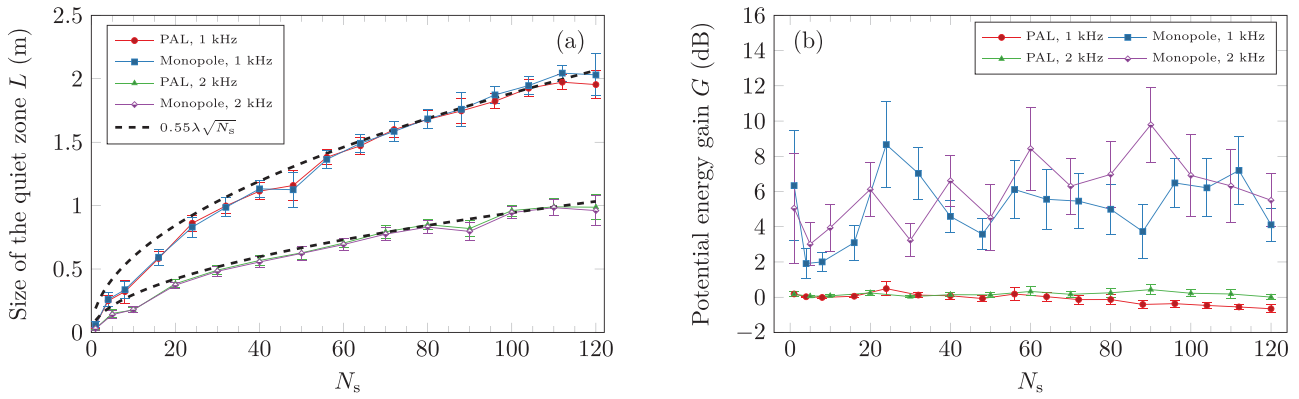
FIG. 10. (Color online) For random 3D primary sound fields under the optimal control with the 3D secondary sources: (a) the quiet zone size as a function of secondary source number; and (b) the potential energy gain as a function of secondary source number. Red circles, PAL at 1 kHz; blue squares, monopole at 1 kHz; green triangles, PAL at 2 kHz; purple diamonds, monopole at 2 kHz; dashed line, $0.55\lambda\sqrt{N_s}$.

size is lower than prediction at higher frequencies when using two PALs. This can be attributed to the fact that the grid separation (5 cm in experiments) of the microphone array is not fine enough to identify the exact quiet zone size. Finally, it is noted that the experiment was done only for the 2D configuration due to the practical difficulties and the number of PALs available. However, over most of the frequency range, the theoretical predictions compare well with the experimental measurements and help to validate the proposed approach to using PALs for ANC.

V. CONCLUSIONS

This paper investigates the remote generation of a large quiet zone in an acoustic free field using multiple PALs in a multichannel ANC system. To simulate a complex primary sound field, multiple point monopoles are located randomly in a 2D plane or 3D space. The simulations show that the quiet zone size generated by N PALs is $0.19\lambda N$ for a wavelength λ when they are uniformly distributed around the circumference of a circle sitting on the same plane as the primary sources; the quiet zone then becomes $0.55\lambda\sqrt{N_s}$ when the PALs are on the surface of a sphere for 3D space. The experimental measurements of the quiet zone with two and four PALs for the 2D configuration are also presented to validate the numerical simulations.

The quiet zone size generated by PALs is found to be similar to that observed with traditional omnidirectional
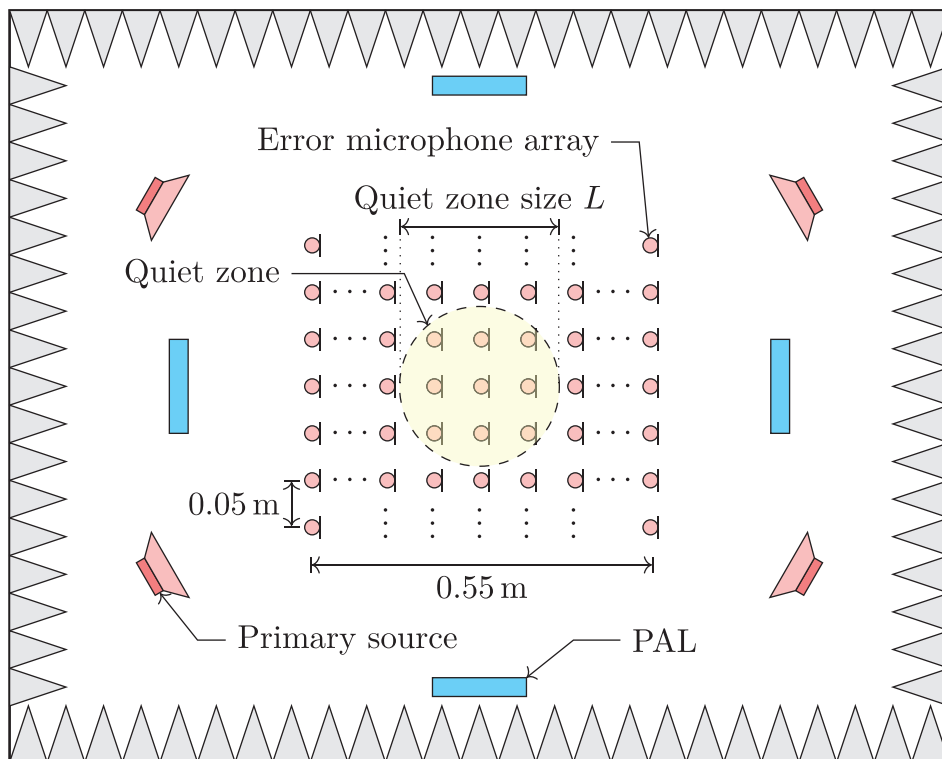

FIG. 11. (Color online) Top view of the experiment setup in a full anechoic room.

J. Acoust. Soc. Am. **151** (2), February 2022
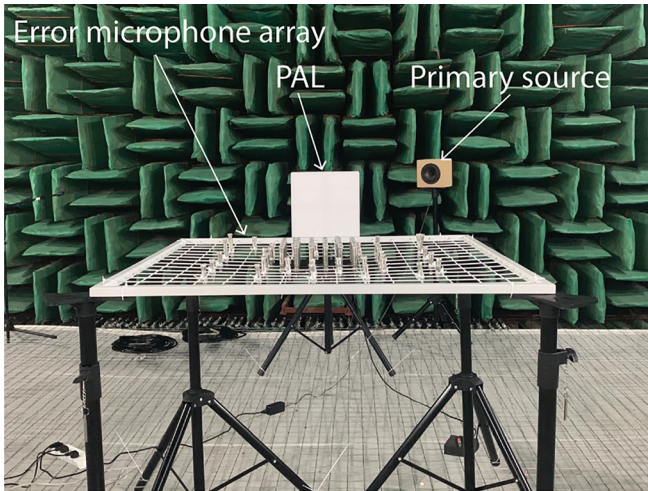
Zhong *et al.*   1243

FIG. 12. (Color online) Photo of the experiment setup in a full anechoic room.

loudspeakers. However, the spillover effects of using PALs as secondary sources are much smaller than traditional loudspeakers, indicating that they can create a larger quiet zone around the target point without affecting other areas. This is because PALs are highly directional loudspeakers, whereas traditional loudspeakers are omnidirectional. Therefore, PALs provide promising secondary sources in multichannel ANC systems, such as a virtual sound barrier system.[30] However, it should be noted that the poor low-frequency response of PALs may limit their use in real applications at low frequencies. Moreover, all of the points inside the target zone to be controlled are chosen here as error points, which requires many error sensors and a high-performance digital signal processor. To reduce the number of error sensors, it is desirable to conduct further studies on the optimal error-sensing strategy when using PALs.
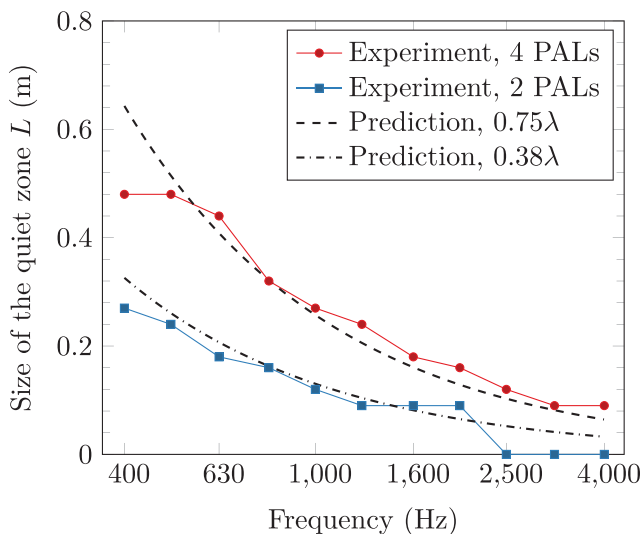

FIG. 13. (Color online) Experimental measurements and predictions for two and four PALs as secondary sources. Red circles, experimental measurements for four PALs; blue squares, experimental measurements for two PALs; dashed line, predictions 0.75λ; dashed-dotted line, predictions 0.38λ.

[1]S. J. Elliott, P. A. Nelson, I. M. Stothers, and C. C. Boucher, "In-flight experiments on the active control of propeller-induced cabin noise," J. Sound Vib. **140**(2), 219–238 (1990).

[2]P. N. Samarasinghe, W. Zhang, and T. D. Abhayapala, "Recent advances in active noise control inside automobile cabins: Toward quieter cars," IEEE Signal Process. Mag. **33**(6), 61–73 (2016).

[3]B. Lam, W.-S. Gan, D. Shi, M. Nishimura, and S. Elliott, "Ten questions concerning active noise control in the built environment," Build. Environ. **200**, 107928 (2021).

[4]Y. Maeno, Y. Mitsufuji, and T. D. Abhayapala, "Mode domain spatial active noise control using sparse signal representation," in *Proceedings of the 2018 IEEE International Conference on Acoustics, Speech and Signal Processing (ICASSP)*, Calgary, Alberta, Canada (April 15–20, 2018), pp. 211-215.

[5]J. Zhang, T. D. Abhayapala, P. N. Samarasinghe, W. Zhang, and S. Jiang, "Multichannel active noise control for spatially sparse noise fields," J. Acoust. Soc. Am. **140**(6), EL510–EL516 (2016).

[6]D. Shi, B. Lam, S. Wen, and W.-S. Gan, "Multichannel active noise control with spatial derivative constraints to enlarge the quiet zone," in *Proceedings of the 2020 IEEE International Conference on Acoustics, Speech and Signal Processing (ICASSP)*, Barcelona, Spain (May 4–8, 2020), pp. 8419–8423.

[7]D. Shi, B. Lam, W.-S. Gan, and S. Wen, "Block coordinate descent based algorithm for computational complexity reduction in multichannel active noise control system," Mech. Syst. Signal Process. **151**, 107346 (2021).

[8]S. J. Elliott, J. Cheer, L. Bhan, C. Shi, and W.-S. Gan, "A wavenumber approach to analysing the active control of plane waves with arrays of secondary sources," J. Sound Vib. **419**, 405–419 (2018).

[9]J. Guo, J. Pan, and C. Bao, "Actively created quiet zones by multiple control sources in free space," J. Acoust. Soc. Am. **101**(3), 1492–1501 (1997).

[10]N. Tanaka and M. Tanaka, "Active noise control using a steerable parametric array loudspeaker," J. Acoust. Soc. Am. **127**(6), 3526–3537 (2010).

[11]Q. Hu and S. K. Tang, "Active cancellation of sound generated by finite length coherent line sources using piston-like secondary source arrays," J. Acoust. Soc. Am. **145**(6), 3647–3655 (2019).

[12]W.-S. Gan, J. Yang, and T. Kamakura, "A review of parametric acoustic array in air," Appl. Acoust. **73**(12), 1211–1219 (2012).

[13]J. Guo and J. Pan, "Effects of reflective ground on the actively created quiet zones," J. Acoust. Soc. Am. **103**(2), 944–952 (1998).

[14]S. J. Elliott, P. Joseph, A. J. Bullmore, and P. A. Nelson, "Active cancellation at a point in a pure tone diffuse sound field," J. Sound Vib. **120**(1), 183–189 (1988).

[15]J. Zhang, T. D. Abhayapala, W. Zhang, and P. N. Samarasinghe, "Active noise control over space: A subspace method for performance analysis," Appl. Sci. **9**(6), 1250 (2019).

[16]N. Epain and E. Friot, "Active control of sound inside a sphere via control of the acoustic pressure at the boundary surface," J. Sound Vib. **299**(3), 587–604 (2007).

[17]H. Zou, X. Qiu, J. Lu, and F. Niu, "A preliminary experimental study on virtual sound barrier system," J. Sound Vib. **307**(1-2), 379–385 (2007).

[18]P. Joseph, S. J. Elliott, and P. A. Nelson, "Near field zones of quiet," J. Sound Vib. **172**(5), 605–627 (1994).

[19]A. David and S. J. Elliott, "Numerical studies of actively generated quiet zones," Appl. Acoust. **41**(1), 63–79 (1994).

[20]G. A. Mangiante, "Active sound absorption," J. Acoust. Soc. Am. **61**(6), 1516–1523 (1977).

[21]W. Chen, W. Rao, H. Min, and X. Qiu, "An active noise barrier with unidirectional secondary sources," Appl. Acoust. **72**(12), 969–974 (2011).

1244   J. Acoust. Soc. Am. **151** (2), February 2022

Zhong *et al.*

[22]L. A. Brooks, A. C. Zander, and C. H. Hansen, "Investigation into the feasibility of using a parametric array control source in an active noise control system," in *Proceedings of Acoustics*, Busselton, Western Australia (November 9–11, 2005), pp. 39-45.

[23]T. Komatsuzaki and Y. Iwata, "Active noise control using high-directional parametric loudspeaker," J. Environ. Eng. **6**(1), 140–149 (2011).

[24]J. Zhong, T. Xiao, B. Halkon, R. Kirby, and X. Qiu, "An experimental study on the active noise control using a parametric array loudspeaker," in *Proceedings of INTERNOISE 2020*, Seoul, Korea (August 23–26, 2020), pp. 662–668.

[25]K. Tanaka, C. Shi, and Y. Kajikawa, "Binaural active noise control using parametric array loudspeakers," Appl. Acoust. **116**, 170–176 (2017).

[26]W.-K. Tseng, "Quiet zone design in diffuse fields using ultrasonic transducers," J. Appl. Math. Phys. **03**(02), 247 (2015).

[27]J. Zhong, R. Kirby, and X. Qiu, "A spherical expansion for audio sounds generated by a circular parametric array loudspeaker," J. Acoust. Soc. Am. **147**(5), 3502–3510 (2020).

[28]M. Červenka and M. Bednařík, "Non-paraxial model for a parametric acoustic array," J. Acoust. Soc. Am. **134**(2), 933–938 (2013).

[29]O. Kirkeby, P. A. Nelson, F. Orduna-Bustamante, and H. Hamada, "Local sound field reproduction using digital signal processing," J. Acoust. Soc. Am. **100**(3), 1584–1593 (1996).

[30]X. Qiu, *An Introduction to Virtual Sound Barriers* (CRC Press, New York, 2019).

[31]M. Červenka and M. Bednařík, "A versatile computational approach for the numerical modelling of parametric acoustic array," J. Acoust. Soc. Am. **146**(4), 2163–2169 (2019).

[32]J. Zhong, R. Kirby, and X. Qiu, "The near field, Westervelt far field, and inverse-law far field of the audio sound generated by parametric array loudspeakers," J. Acoust. Soc. Am. **149**(3), 1524–1535 (2021).

[33]N. J. A. Sloane, R. H. Hardin, and W. D. Smith, "Spherical Codes: Nice arrangements of points on a sphere in various dimensions," http://neilsloane.com/packings/dim3/ (Last viewed August 22, 2021).

[34]F. Farias and W. Abdulla, "On Rayleigh distance and absorption length of parametric loudspeakers," in *Proceedings of the 2015 Asia-Pacific Signal and Information Processing Association Annual Summit and Conference (APSIPA)*, Hong Kong (December 16–19, 2015), pp. 1262-1265.

[35]ISO 9613-1:1993: *Acoustics—Attenuation of Sound during Propagation Outdoors—Part 1: Calculation of the Absorption of Sound by the Atmosphere* (International Organization for Standardization, Genève, 1993).

[36]J. Zhong, S. Wang, R. Kirby, and X. Qiu, "Insertion loss of a thin partition for audio sounds generated by a parametric array loudspeaker," J. Acoust. Soc. Am. **148**(1), 226–235 (2020).

[37]P. A. Nelson and S. J. Elliott, *Active Control of Sound* (Academic Press Inc., San Diego, 1992).

[38]P. Ji and J. Yang, "An experimental investigation about parameters' effects on spurious sound in parametric loudspeaker," Appl. Acoust. **148**, 67–74 (2019).